ディーゼル燃焼場におけるすす粒子生成過程とTime-Resolved LIIによる火炎中すす粒子計測

1. 背景＆研究目的
2. 化学反応動力学によるすす生成過程の解析
3. LIIによる燃焼火炎場のすす粒子測定

同志社大学大学院　工学研究科　千田　二郎

2006.3.13

Recent Research Attempts against the Emission Regulation

Recently…

More regulation on particle matter emission from diesel engine is gradually conducted

Regulation on particulate matter emissions from diesel vehicles

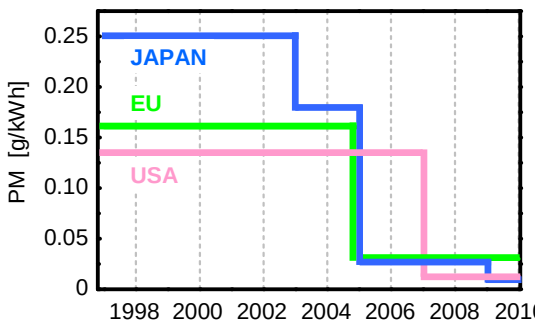

Emission reduction approaches

-Improving atomization and turbulent mixing
- High pressure fuel injection
- small orifice nozzle

-Combustion Method
- HCCI
- MK Combustion
- Low temp. rich combustion

-Fuel modification
- Oxgenated fuels
- Biodiesel fuels

-Aftertreatment technologies
- DPF

Back ground of this study

Nanoparticles (d_p<50nm)
ex.) Soot, SOF

→ **Serious health damage**
- Lung cancer
- breathing problem

High number concentration
due to low mass concentration
→Nanoparticles is unregulated

Typical particle diameter distribution

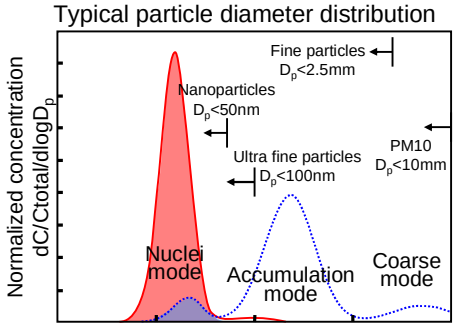

Objectives
- **Investigate soot formation characteristic focused on soot volume fraction and particle diameter in diesel spray flame**
- **Investigate effects of various parameters on particulate characteristics**

Soot Formation Processes in Detailed Model

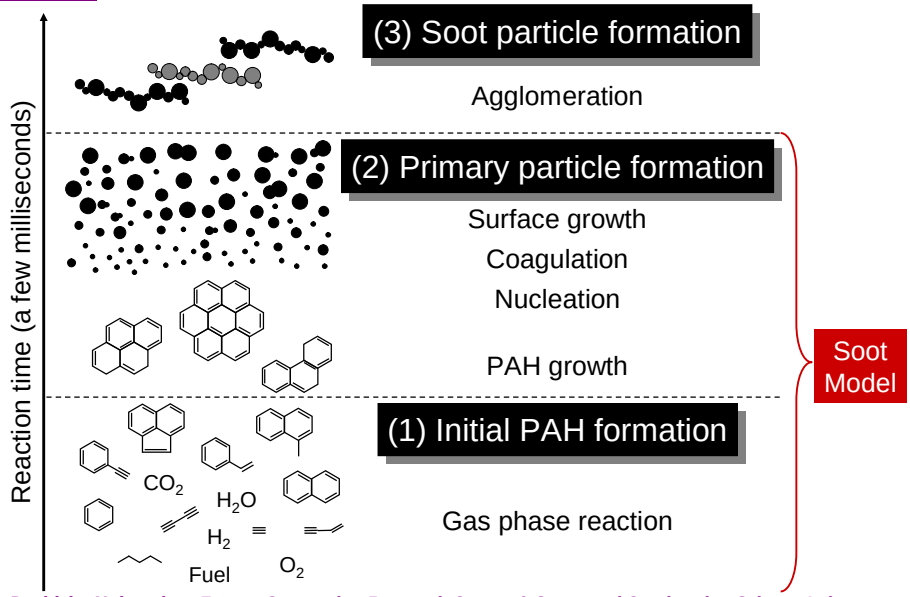

Conceptual Model of Diesel Jet Flame
(Dec, SAE Paper 970873, 1997)

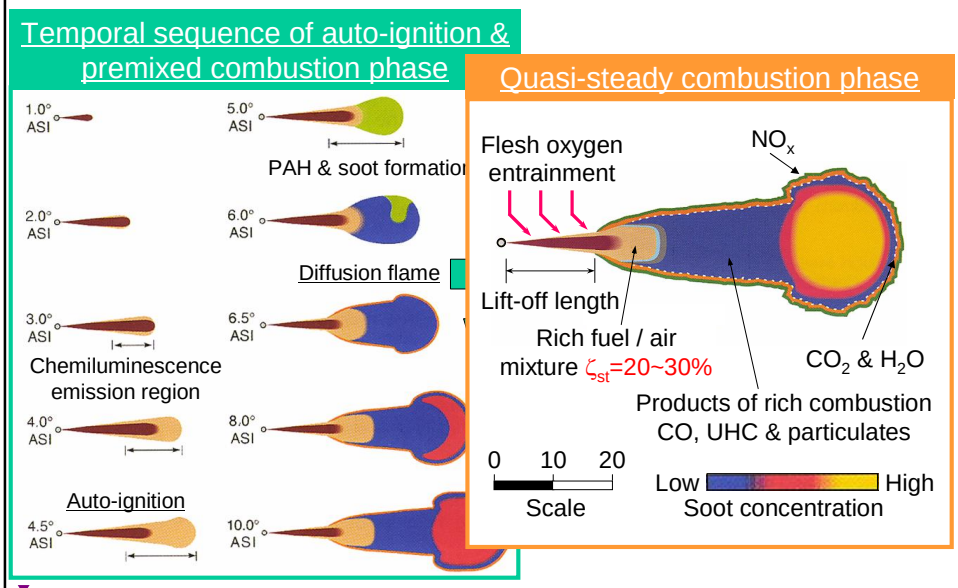

Conceptual model of diesel combustion by Aizawa/Kosaka/Kamimoto in TIT

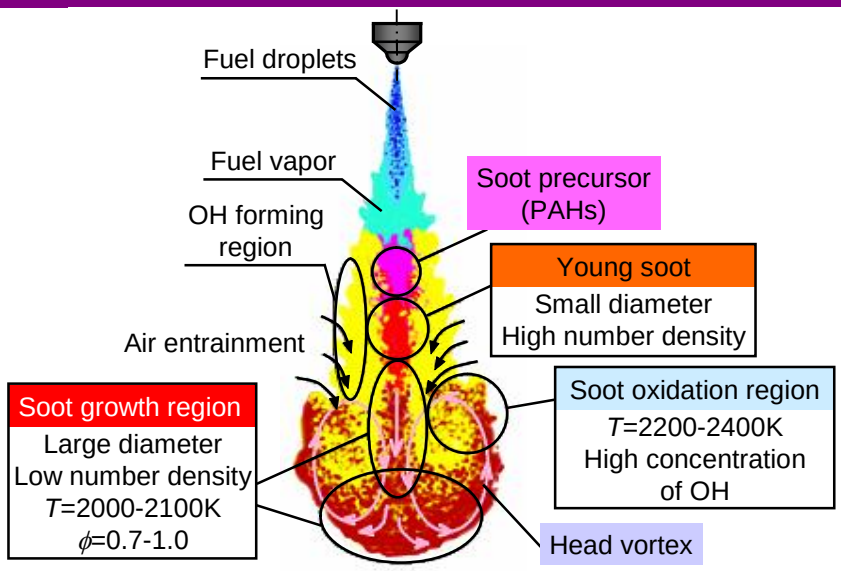

Distribution of soot volume fraction and soot particle diameter in diesel jet flame obtained by Time-resolved LII

fuel: n-heptane, T_{amb}=900[K], ρ_{amb}=16.2[kg/m³], X_{O2}=17%, ΔP_{inj}=70[MPa]

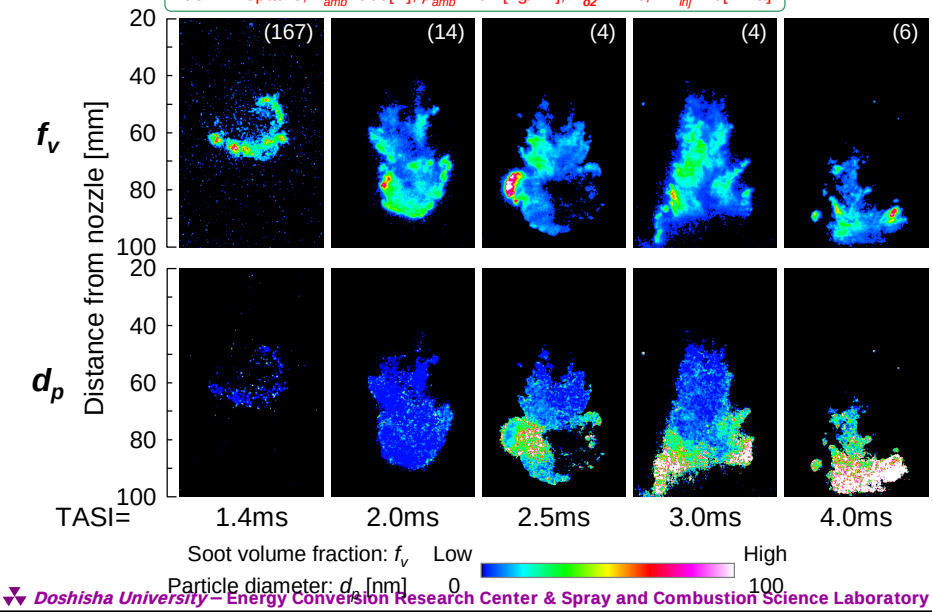

Combustion Mode in Φ – T Map

Low temp. rich combustion [Akihama et al., SAE Paper 2001-01-0655]

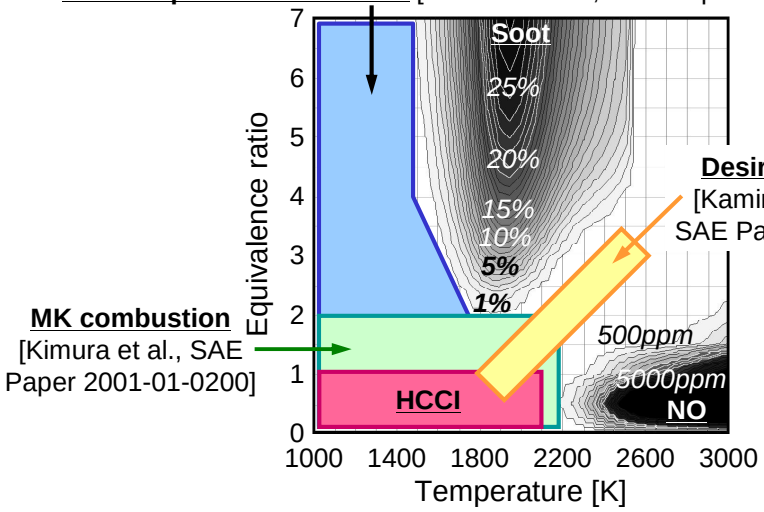

Desirable path
[Kamimoto et al., SAE Paper 880423]

MK combustion
[Kimura et al., SAE Paper 2001-01-0200]

非定常噴霧燃焼場のすす粒子生成挙動の解析

含酸素燃料を用いた無煙ディーゼル燃焼法の化学反応論的解析

- Detailed Chemical Kinetic Modeling
of Smokeless Diesel Combustion
with Oxygenated Fuels –

北村･伊藤ら

Oxygen Impact on Particulate Emissions

(Miyamoto et al., Int. J. Engine Research, 1-1, pp.71-85, 2000)

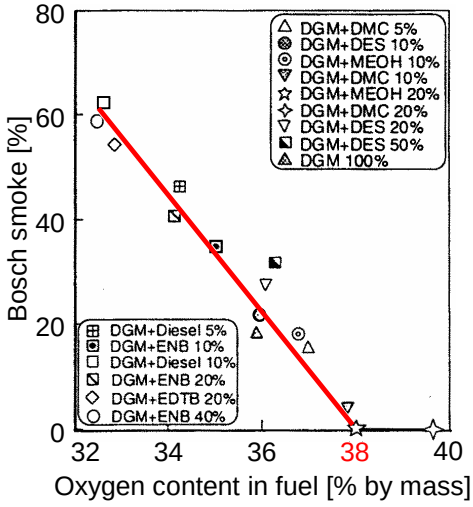

Main Oxygenate
DGM: $[CH_3OCH_2CH_2]_2O$

Operating Condition
ϕ_{all} = 1.0
EGR ratio: 30 vol%

Using highly oxygenated fuel
1. Stoichiometric
2. Non-sooting
combustion can be realized!!

Reaction Model of Soot Formation

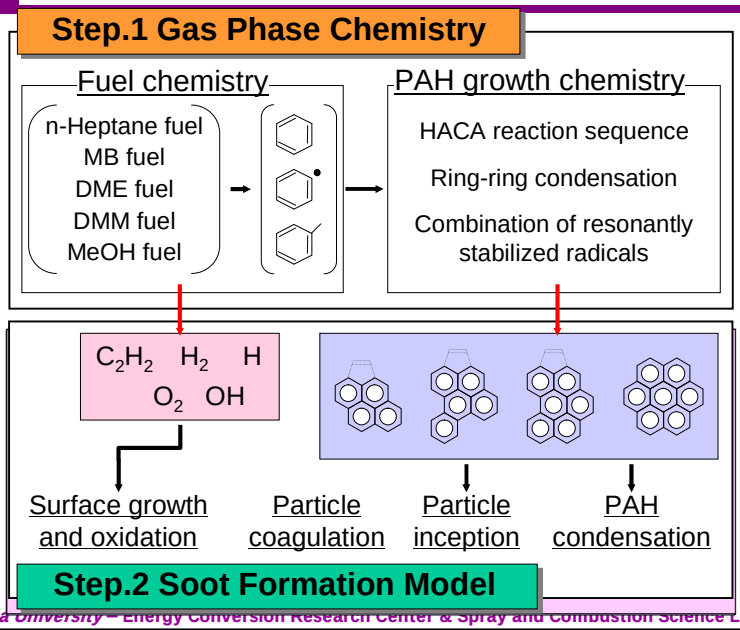

Gas Phase Chemistry – 素反応モデル

Chemkin-III SENKINコード
→低温酸化・高温酸化・熱分解～7環PAH生成ﾓﾃﾞﾙ
・n-ヘプタン反応モデル—Curranらのモデル
・MarinovらのPAH生成ﾓﾃﾞﾙ (C4以下の低級炭化水素から4環芳香族までの分子成長反応
・CurranらのDMEﾓﾃﾞﾙ、Marinovらのｴﾀﾉｰﾙﾓﾃﾞﾙ
・Fisherらのﾒﾁﾙﾌﾞﾀﾉｴｰﾄ酸化反応ﾓﾃﾞﾙ
・Dalyらのｼﾞﾒﾄｷｼﾒﾀﾝ酸化反応ﾓﾃﾞﾙ

→すす粒子生成ﾓﾃﾞﾙはFrenklachらのﾓｰﾒﾝﾄ法による粒子生成ﾓﾃﾞﾙ
・HACAﾒｶﾆｽﾞﾑ-芳香族環への水素引抜き-ｱｾﾁﾚﾝ付加反応
・FrenklachらのPAH生成ﾓﾃﾞﾙ

Expression of soot yield, particle diameter and soot volume fraction

Particle number $N_{soot} = M_0$

Soot yield $SY = \frac{M_1}{m_{ini}}$

Particle diameter $d_{soot} = \left(\frac{6 m_c}{\pi \rho_{soot}} \cdot \frac{M_1}{M_0} \right)^{1/3}$

Soot volume fraction $F_v = \frac{\pi d_{soot}^3}{6} \cdot M_0$

Model Validation I: Temperature Dependence of Soot Formation

(fuel: benzene, ϕ=5, p=3 MPa, reaction time: t=0.1~1.2 ms)

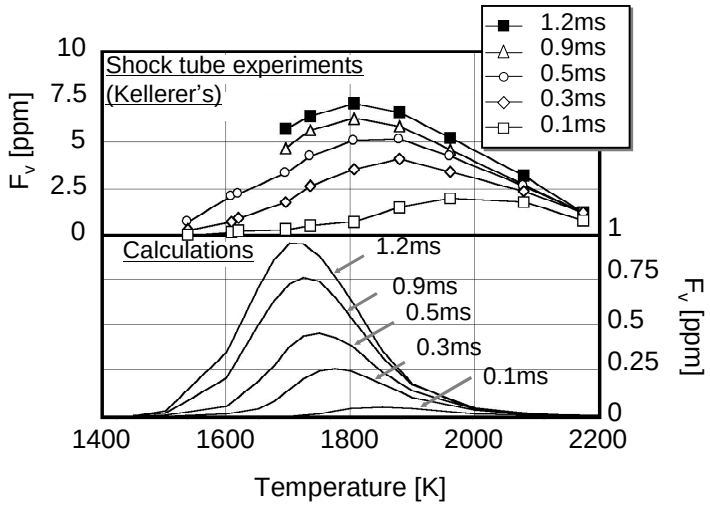

Model Validation II: Pressure Dependence of F_v, d_{soot}, N_{soot}

(fuel: toluene, ϕ=5, T=1600 K, p=3 MPa, reaction time: t=1.5 ms)

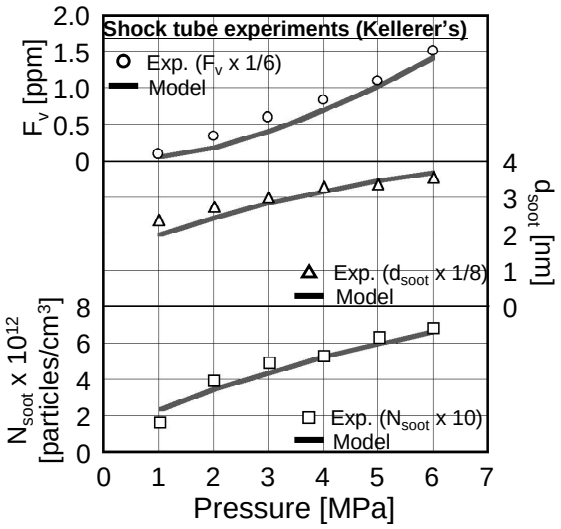

Model Validation III: Sooting Limit on Equivalence Ratio - Temperature Diagram

(fuel: toluene, p=0.5 MPa, reaction time: t=4.0 ms)

Experiments
= Wang , et al.

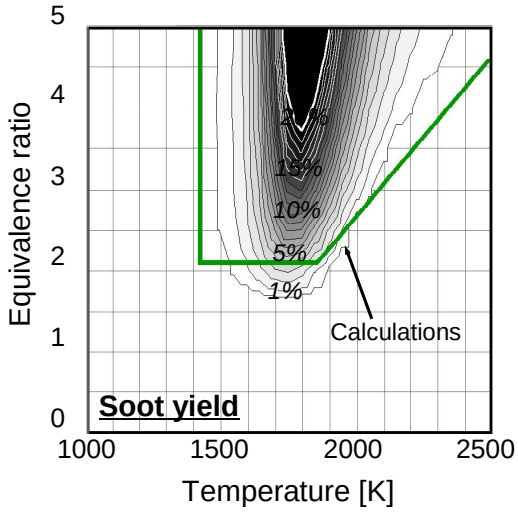

Fuel Consumption Process in n-Heptane and DME Reactions (T=900 K, p=8 MPa, ϕ=4)

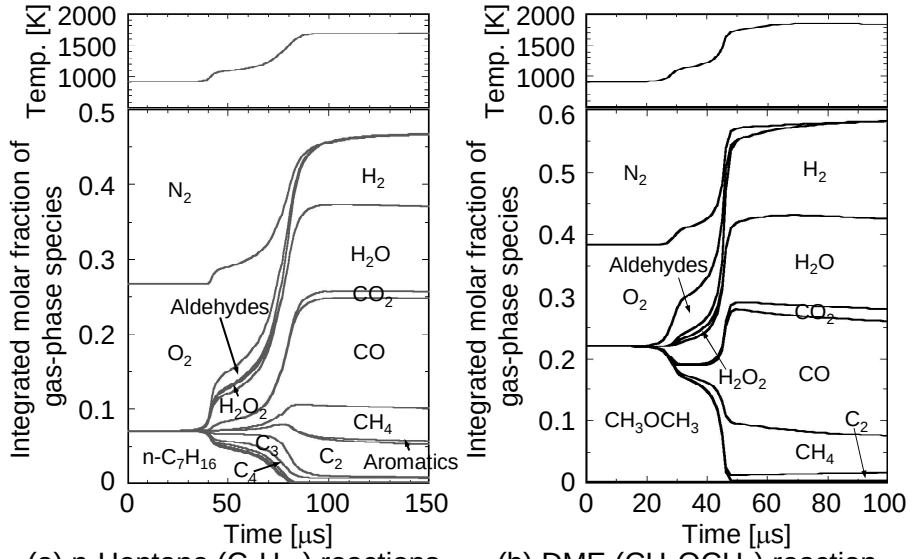

(a) n-Heptane (C_7H_{16}) reactions (b) DME (CH_3OCH_3) reaction

Chemical Role of Oxygenated Fuels on PAH Suppression

これまでの含酸素燃料の基礎解析によると、PAH生成
およびその前駆物質であるC2,C3などの低級炭化水素生成
の抑制特性として、燃料構造が影響する。

① 主要反応生成物が重要
アセチレン、エチレンなどの多環化物質は促進
アルデヒド類は抑制に働く

② 酸素原子に由来するOHラジカルによる酸化
→分子成長反応を抑制

③ アルデヒド類はHCOラジカルを介して水素原子を生成
→ベンゼン前駆体のﾌﾟﾛﾊﾟﾙｷﾞﾙﾗｼﾞｶﾙの水素引き抜き
→ベンゼン生成を抑制

Oxygenated Fuels Examined

Oxygenates (Code name)	Molecular equation	Oxygen content [% by mass]
Methanol (MeOH)	CH_3OH	50
Dimethoxy methane (DMM)	$CH_3OCH_2OCH_3$	42.1
Dimethyl ether (DME)	CH_3OCH_3	34.8
Methyl butanoate (MB)	$CH_3(CH_2)_2(CO)OCH_3$	31.4

Effect of Fuel Type on PAH Formation

(p=10 MPa, [C]=4.21x10^{19}~1.26x10^{20} atoms/cm^3 ,
reaction time: t= 3ms, isometric pyrolysis reaction)

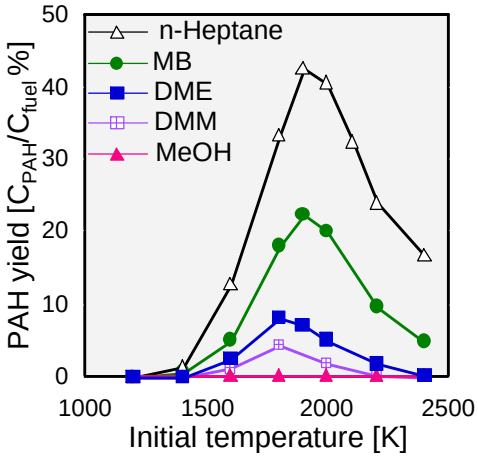

(a) PAH yield (1000 ~ 2400 K)

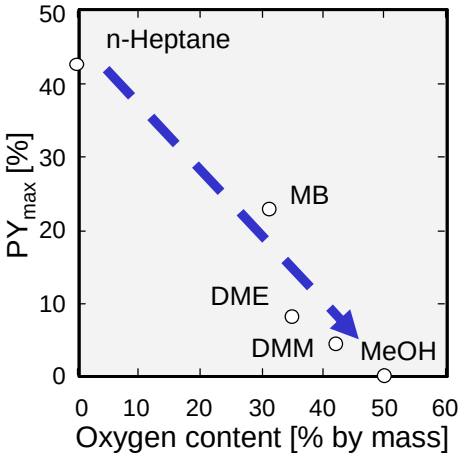

(b) PAH yield (bell peak temp.)

Chemical Role of Molecular Oxygen and Oxygenate on PAH Suppression

＊すす生成のベル型温度依存性

- 低温域では熱分解による低級不飽和炭化水素の生成が遅れ、PHA抑制
- 高温域では分子成長反応の逆反応であるPAHの分解可能が促進

➔ギブス生成自由ｴﾈﾙｷﾞの観点でも、1500K以上ではPAHよりｱｾﾁﾚﾝなどの低級不飽和炭化水素が安定

＊ベル型分布のリーン側での低温側シフト（外部酸素）

- 燃料の酸化反応の寄与度が増加し、初期に900K程度の低温でも酸化後の平衡温度が1600-1700Kに達する

＊ﾃﾞｨｰｾﾞﾙ噴霧火炎内部でのすす生成の推定

- 低燃料噴射圧力条件：低い空気導入率
  - →最大PAH生成温度域は1700K程度の高温
  - →噴霧外縁部の拡散火炎近傍ですす生成
- 高燃料噴射圧力条件：高い空気導入率
  - →噴霧内部の当量比4程度の希薄な領域で900-1000KでPAH最大生成
  - →噴霧中心部で活発なすす生成が生じる

Particle Number Density Map as a Function of ϕ and T for Three Fuels

(P=6 MPa, reaction time: t=2 ms)

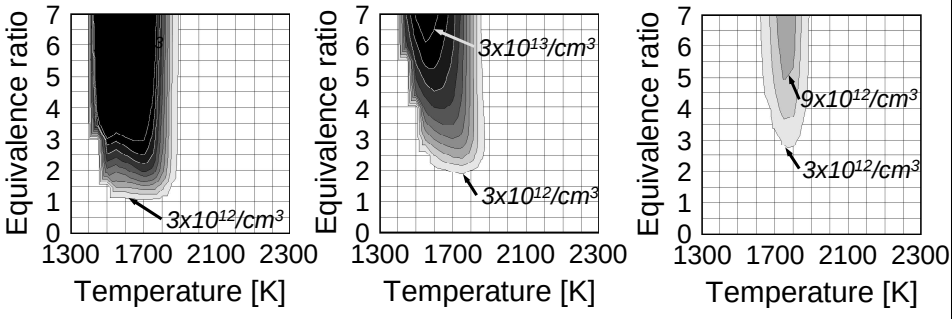

(a) Benzene reactions (b) n-Heptane reactions (c) DME reactions

Particle Number Density Map as a Function of ϕ and T for Three Fuels

(P=6 MPa, reaction time: t=2ms)

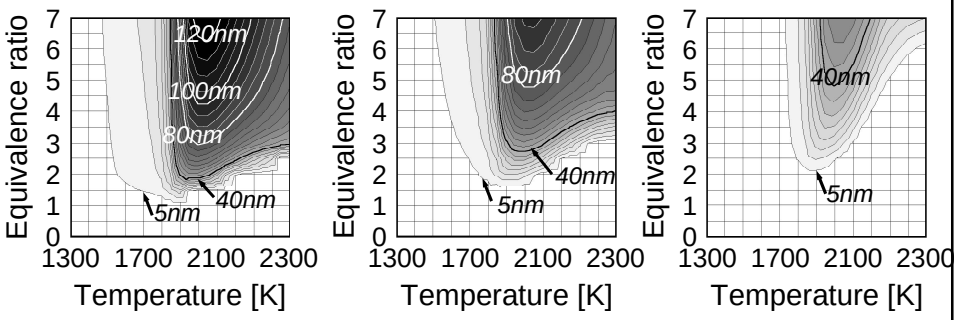

(a) Benzene reactions (b) n-Heptane reactions (c) DME reactions

Variation of Soot Formation Limits among Different Type of Fuels on ϕ-T Diagram

(defined as 1% soot yield)

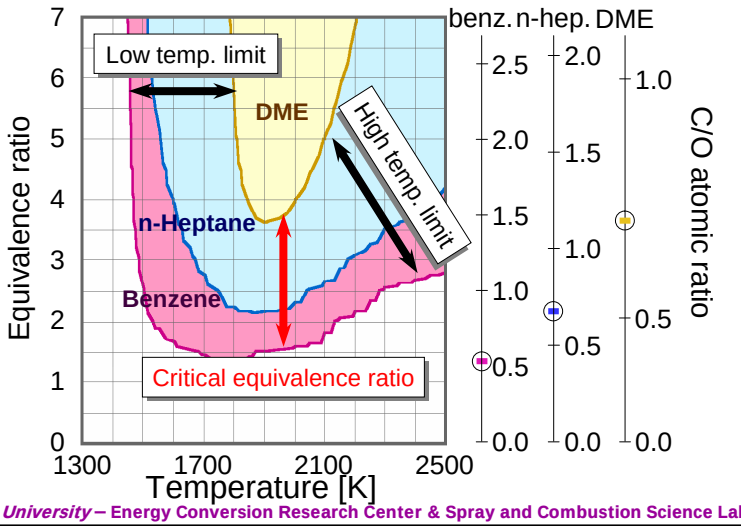

Conclusions

詳細な0次元すす反応動力学モデルにより，粒子径･粒子数を考慮したすす生成の当量比-温度マップ解析および燃料組成がすす生成特性に及ぼす影響の検討を行ない，以下に示す知見を得た．

- すす体積分率のベルピーク温度よりも低温側では，小粒径･高数密度･高PAH濃度の粒子が，逆に高温側では，大粒径･低数密度･低PAH濃度の粒子が生成される．
- 上記に起因して，すす排出重量の低減に加え，微小すす粒子数および未燃PAH濃度を同時に低減するには，当量比-温度マップ上におけるすす生成半島の低温側より，燃料希薄側の利用が望まれる．
- すす生成の当量比-温度依存性は燃料成分の影響を強く受ける．特に，含酸素燃料では最大すす生成収率の大幅な低下やすす生成領域の大幅な縮小化が可能となる．

Turbulence chemistry interaction model

(Kong et al. SAE paper 2001-01-1026)

- Production rate of species i

$$\omega_i = \frac{Y_i^* - Y_i}{\tau_{kin,i} + f\tau_{turb}}$$

Y_i : current concentration
Y_i^*: equilibrium concentration
$\tau_{kin,i}$: kinetic timescale
τ_{turb} : turbulent timescale〜k/ε
f : delay coefficient

- Kinetic controlled production rate of species i

$$\omega_{kin,i} = \frac{Y_i^* - Y_i}{\tau_{kin,i}} = \frac{Y_i' - Y_i}{dt} = \frac{\Delta Y_i}{dt}$$

Y_i : current concentration
Y_i' : concentration after CHEMKIN cal.
dt : numerical time-step

$$\tau_{kin,i} = \frac{Y_i^* - Y_i}{\Delta Y_i} dt$$

＊Assumptions

$$\left.\begin{array}{l}\tau_{kin,i} = \tau_{kin,\,fuel} \\ Y_f^* \to 0\end{array}\right\} \Rightarrow \left\{\begin{array}{l}\tau_{kin} = (-Y_f / \Delta Y_f)dt \\ Y_i^* - Y_i = (-Y_f / \Delta Y_f)\Delta Y_i\end{array}\right.$$

New species at the current time-step

$$Y_i^{n+1} - Y_i^n = \omega_i dt = \frac{(-Y_f / \Delta Y_f)\Delta Y_i}{\tau_{kin} + f\tau_{turb}} dt$$

$$= \frac{\tau_{kin}}{\tau_{kin} + f\tau_{turb}} \Delta Y_i$$

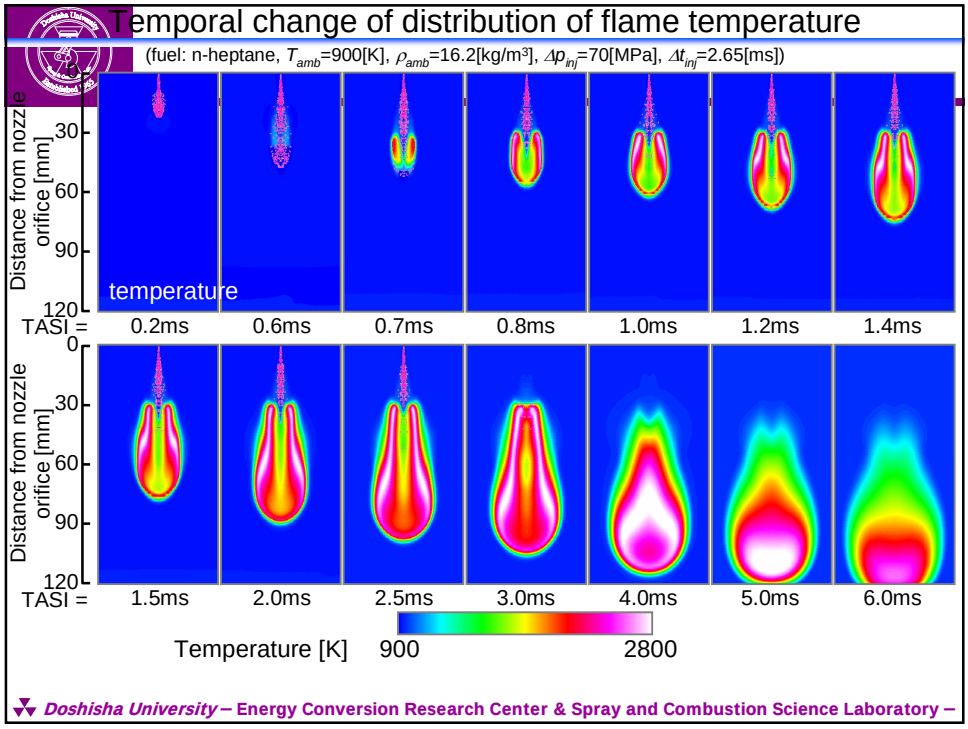
Temporal change of distribution of flame temperature
(fuel: n-heptane, T_{amb}=900[K], ρ_{amb}=16.2[kg/m³], Δp_{inj}=70[MPa], Δt_{inj}=2.65[ms])
Distance from nozzle orifice [mm]
0
30
60
90
120
temperature
TASI =
0.2ms
0.6ms
0.7ms
0.8ms
1.0ms
1.2ms
1.4ms
1.5ms
2.0ms
2.5ms
3.0ms
4.0ms
5.0ms
6.0ms
Temperature [K]
900
2800
Doshisha University – Energy Conversion Research Center & Spray and Combustion Science Laboratory –

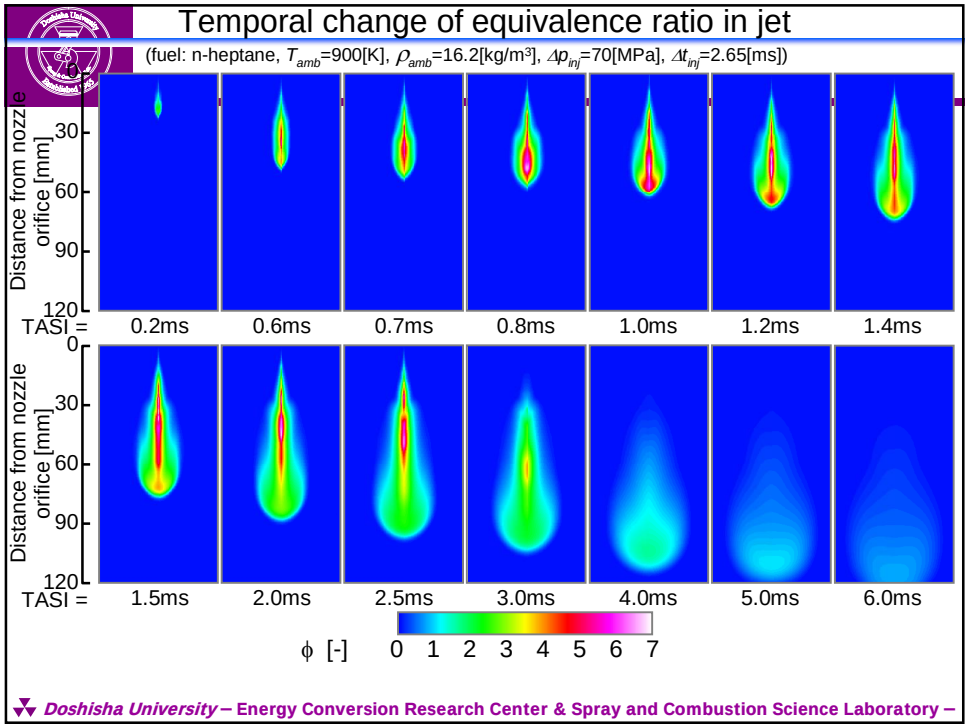
Temporal change of equivalence ratio in jet
(fuel: n-heptane, T_{amb}=900[K], ρ_{amb}=16.2[kg/m³], Δp_{inj}=70[MPa], Δt_{inj}=2.65[ms])
Distance from nozzle orifice [mm]
0
30
60
90
120
TASI =
0.2ms
0.6ms
0.7ms
0.8ms
1.0ms
1.2ms
1.4ms
1.5ms
2.0ms
2.5ms
3.0ms
4.0ms
5.0ms
6.0ms
ϕ [-]
0 1 2 3 4 5 6 7
Doshisha University – Energy Conversion Research Center & Spray and Combustion Science Laboratory –

Distribution of naphthalene mass fraction and soot volume fraction

(fuel: n-heptane, T_{amb}=900[K], ρ_{amb}=16.2[kg/m³], Δp_{inj}=70[MPa], Δt_{inj}=2.65[ms])

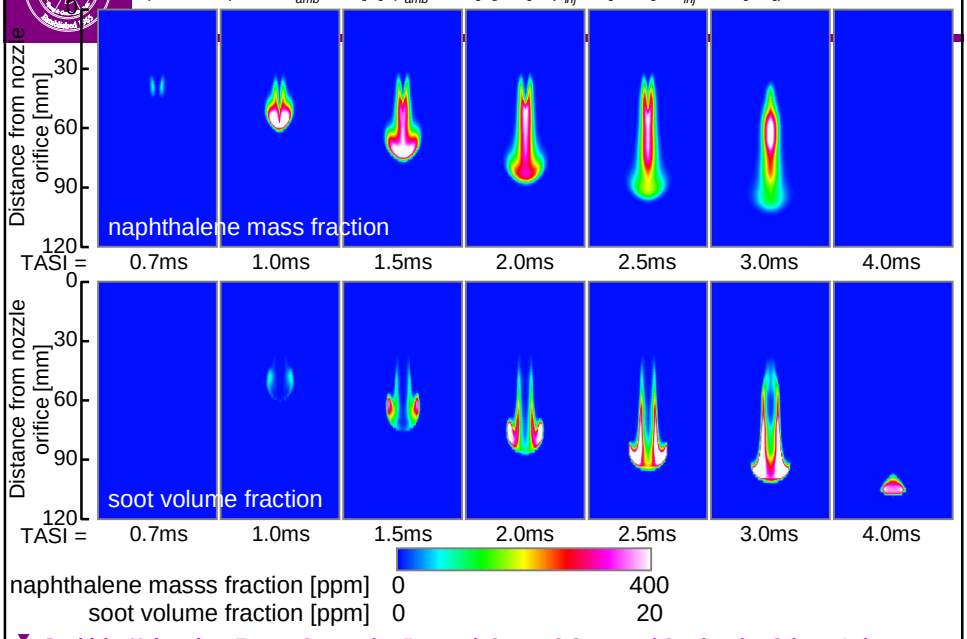

naphthalene masss fraction [ppm] 0 400

soot volume fraction [ppm] 0 20

Soot Measurement Scheme

Soot measurement

Soot volume fraction and soot particle diameter
in a combusting diesel jet

Laser-Induced Incandescence

↓

Soot volume fraction : f_v

Time-resolved LII

↓

Soot particle diameter : d_p

Principle of LII

Laser-Induced Incandescence (LII)

Soot particle temperature increases rapidly
by high energy laser

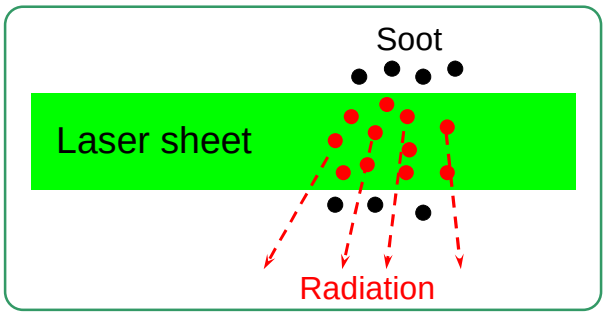

Soot incandescence (LII signal) irradiates
→Visualization of soot distribution

In addition, LII signal intensity $\propto f_v$

Previous Study about Laser Induced Incandescence

A.C.Eckbreth

Fundamental properties of LII

- LII signal intensity increase with increasing laser power
- Decrease in soot diameter due to soot vaporization

L.A.Melton

Numerical analyze of LII

- LII signal intensity is proportional to soot volume fraction

$$F_v \propto N_p \cdot d_p^3$$

Application of LII to diesel engine

J.E.Dec

Advantage of LII for soot diagnostics

- Lack of scattering influence due to droplet or cylinder wall

Theoretical Equations

$$Q_{abs} = \frac{8\pi a E_{(m)}}{\lambda}$$

$$q_{rad} = 4\pi a^2 \varepsilon \sigma (T^4 - T_{flame}^4)$$

LII signal (S_{LII})

$$S_{LII} = \frac{2\pi c_0^2 h}{\lambda_{em}^5 [\exp(hc_0 / \lambda_{em} kT) - 1]} N_p 4\pi a^2 \varepsilon \Delta\lambda$$

At maximum temperature of soot particle (by Melton[#])

$$S_{LII} = N_p \cdot d_p^{\,3+154/\lambda_{em}} \cong N_p \cdot d_p^{\,3} \propto f_v$$

([#] L. A. Melton, APPLIED OPTICS, Vol.23, No.13, pp.2201-2208, 1984)

Time-Resolved LII

- LII signal decay after laser incident depends on particle diameter.
- LII signal ratio at two different times also depends on particle diameter.

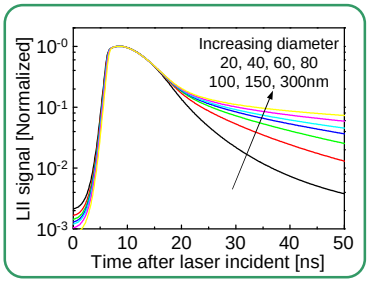

- Temporal change in LII signal decay after laser incident
  (LII signal ratio at two different timing, etc)

Numerical simulation

as well as Melton's method
(L. A. Melton, APPLIED OPTICS, Vol.23, No.13, pp.2201-2208, 1984)

Laser-Induced Incandescence (LII)法の原理

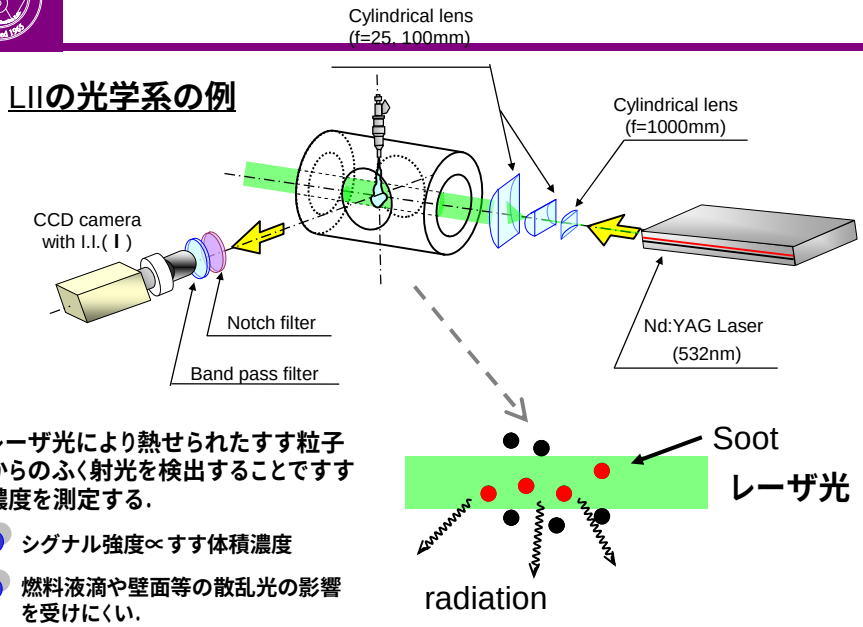

レーザ光により熱せられたすす粒子からのふく射光を検出することですす濃度を測定する.

- シグナル強度∝すす体積濃度
- 燃料液滴や壁面等の散乱光の影響を受けにくい.

Ratio of black body radiation at 4500K an that at 2200K

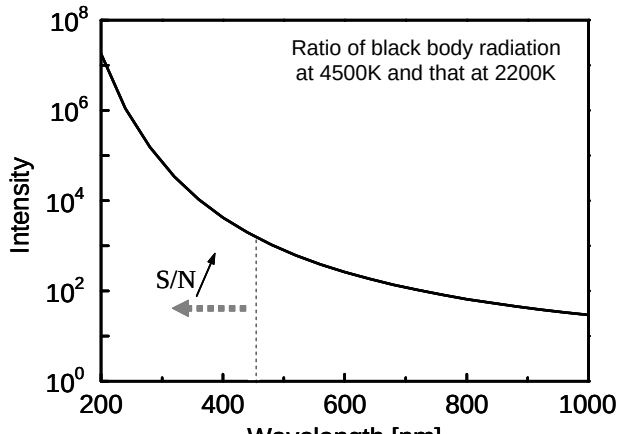

- 短波長ほどS/N比が高い.
- 短波長ほどLII信号強度そのものも低い
- LII信号強度 ∝ $N_p d_p^{3+154nm/\lambda}$ → 長波長ほど体積濃度に比例

LIIシグナル強度に及ぼすレーザ強度の影響

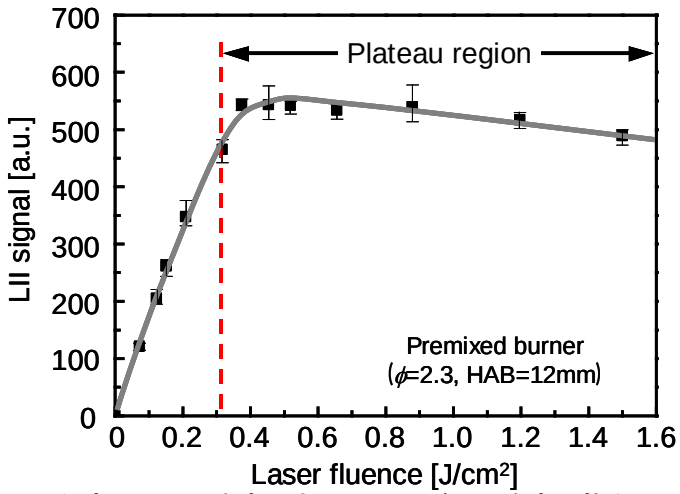

- ある程度のレーザ強度以上ではLIIシグナル強度は飽和する.
  → レーザシート光の強度ムラやすすによるレーザ強度の減衰の影響を受け難い.

LIIを用いたすす粒子径の計測: Time-Resolved LII (TIRE-LII)

- レーザ照射後のLIIシグナル強度の時間履歴は粒子直径に依存する.
- 異なる2時期でのLIIシグナル強度比から粒子直径を算出できる.

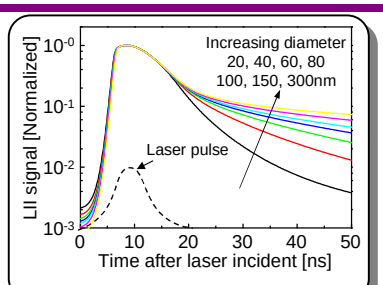

ディーゼル燃焼場 → 高温, 高圧

→ 粒子径が既知の粒子を用いた検定実験が困難.

↓

仮定： 単一球形粒子

↓

LIIシグナルの時間変化を数値予測

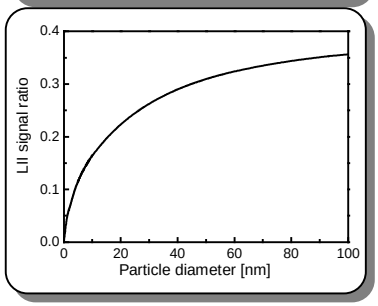

Power balance of a laser-heated soot particle

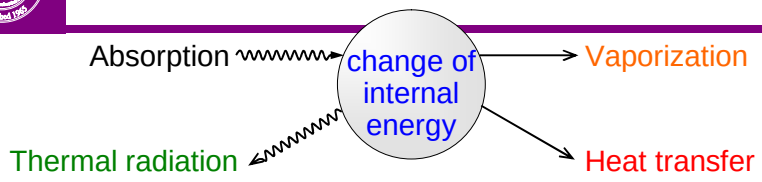

Energy balance equation

$$K_{abs}\pi a^2 q_{(t)} - 4\pi a^2 (T - T_0)\Lambda - \frac{\Delta H_v}{W_s}\cdot\frac{dM}{dt} - q_{rad} - \frac{4}{3}\pi a^3 \rho_s C_s \frac{dT}{dt} = 0$$

absorbed laser energy	heat transfer loss	heat loss soot evaporation	heat loss thermal radiation	internal energy change

Mass conservation equation

$$\frac{dM}{dt} = 4\pi a^2 \rho_s \frac{da}{dt} = 4\pi a^2 \rho_v \sqrt{\frac{RT}{2W_v}}$$

(Stefan Will, et al, APPLIED OPTICS, Vol.37, No.24, pp.5647-5658, 1998)

すす粒子の温度および粒子径変化
(初期粒径: 50nm, 粒子初期温度: 2200K, レーザ強度: 0.92J/cm²)

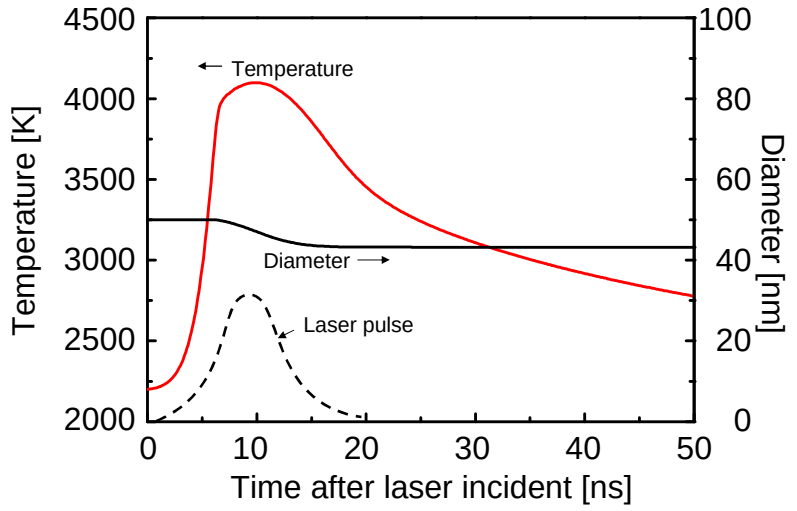

LIIシグナル強度の時間履歴

(初期粒径: 50nm, 粒子初期温度: 2200K, 雰囲気圧力:4.1MPa, レーザ強度: 0.92J/cm^2)

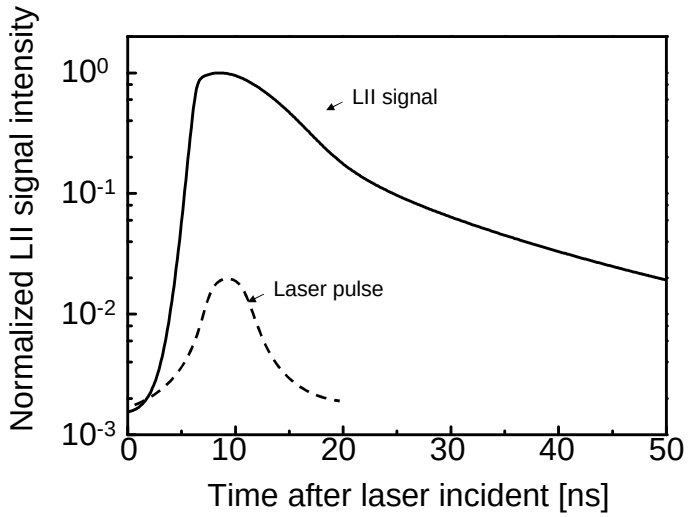

LII signal decay for various particle sizes

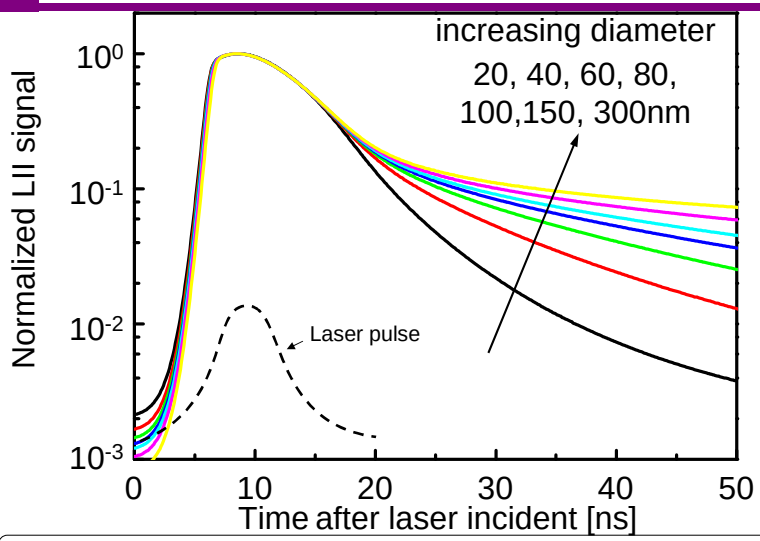

P_{amb}=4.1MPa, Laser fluence=0.92J/cm^2, T_{flame}=2200K

LII signal decay for various particle sizes

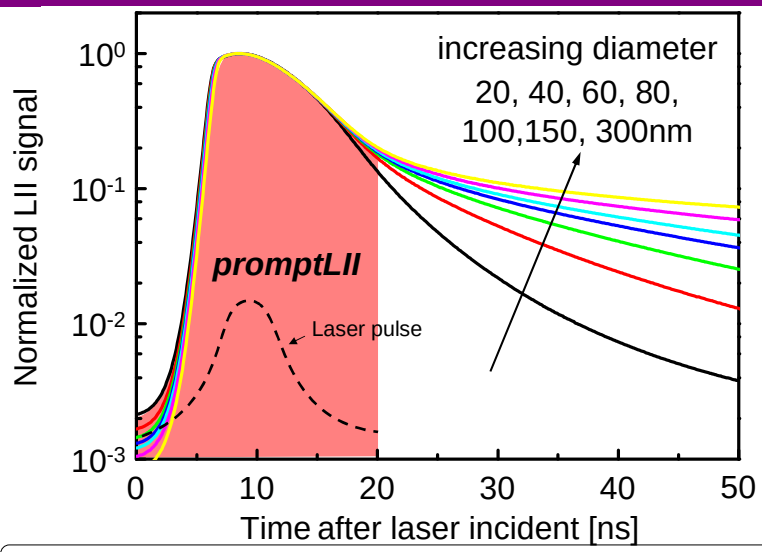

P_{amb}=4.1MPa, Laser fluence=0.92J/cm^2, T_{flame}=2200K

LII signal decay for various particle sizes

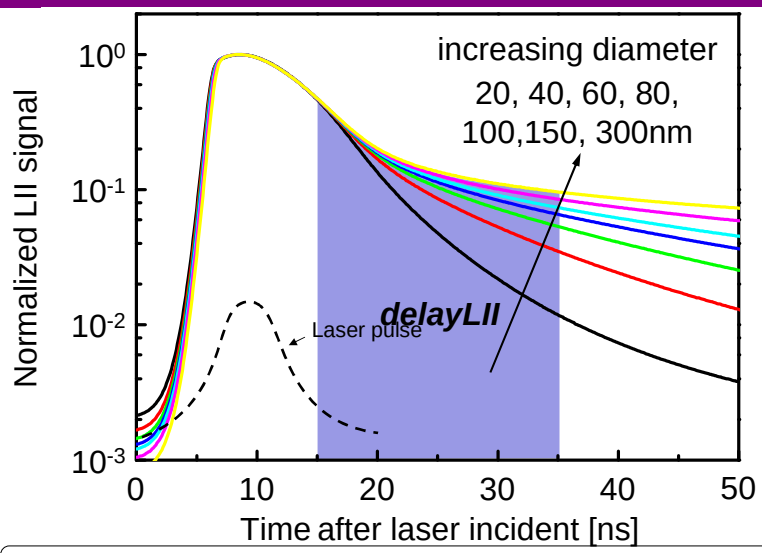

P_{amb}=4.1MPa, Laser fluence=0.92J/cm^2, T_{flame}=2200K

Doshisha University – Energy Conversion Research Center & Spray and Combustion Science Laboratory –

LII signal ratio of first and second gate versus particle diameter

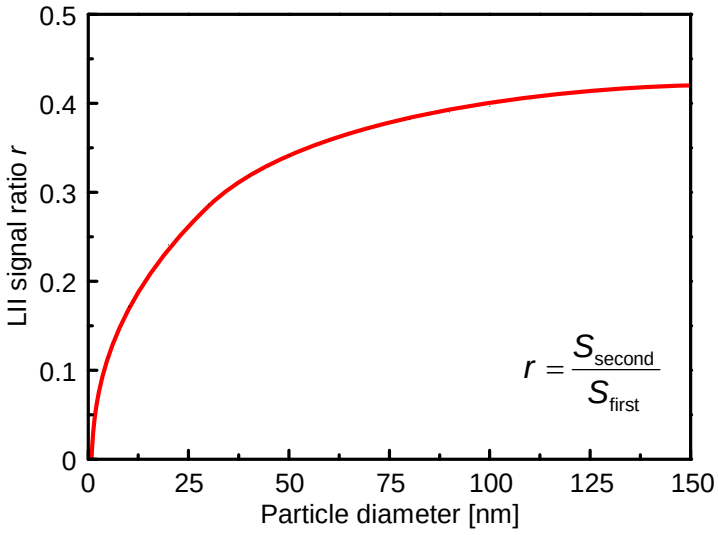

P_{amb}=4.1MPa, Laser fluence=0.67J/cm², T_{flame}=2200K

Time-Resolved LIIによるすす粒子径の決定法

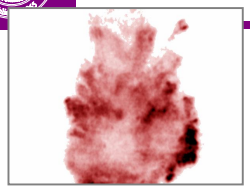

promptLII (raw image)

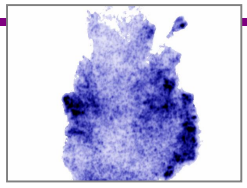

delayLII (raw image)

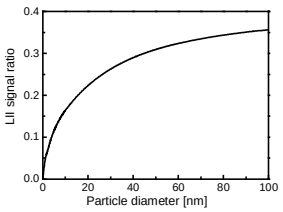

1) $\frac{delayLII}{promptLII}$

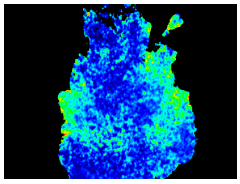

2) From signal ratio to diameter

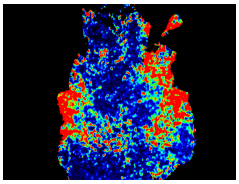

シグナル比を算出

Diameter distribution

LIIシグナルの時間履歴に及ぼす雰囲気圧力の影響

大気圧場では，LIIシグナルの減衰は緩慢である．

→ 大気圧バーナやエンジン排気中のPM粒径を計測する場合は
レーザ照射後数百ns後のシグナルを用いるのが一般的．

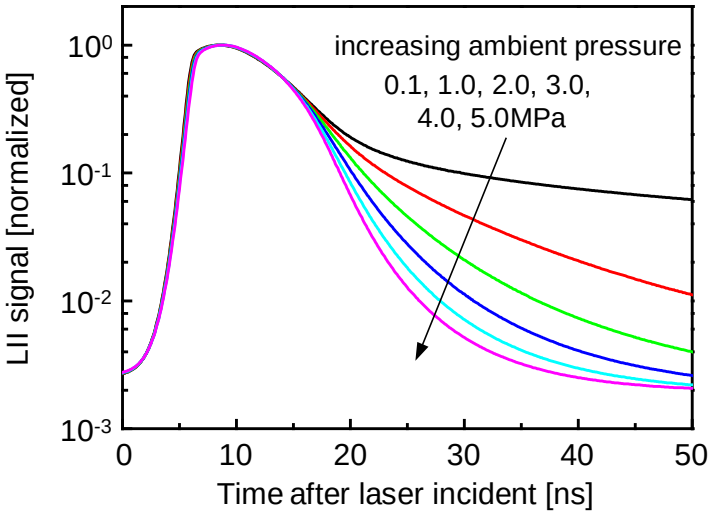

Schematic diagram of experimental system

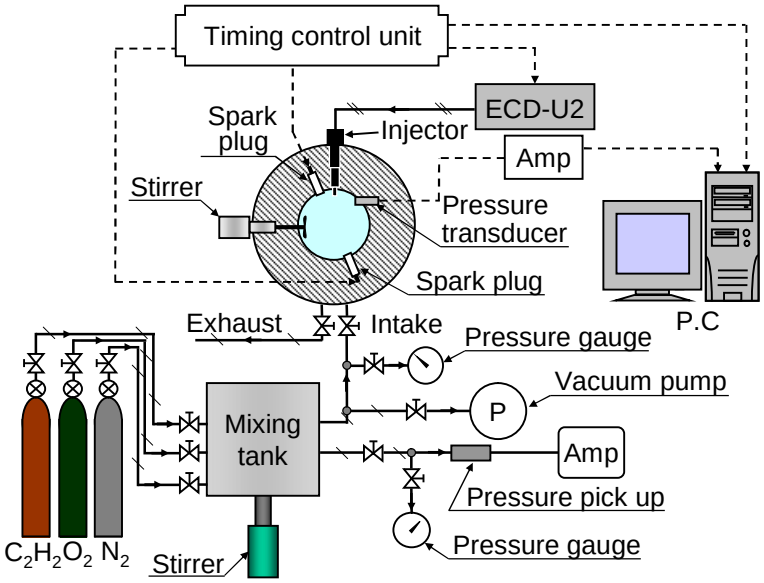

Optical measurement system for Time-resolved LII

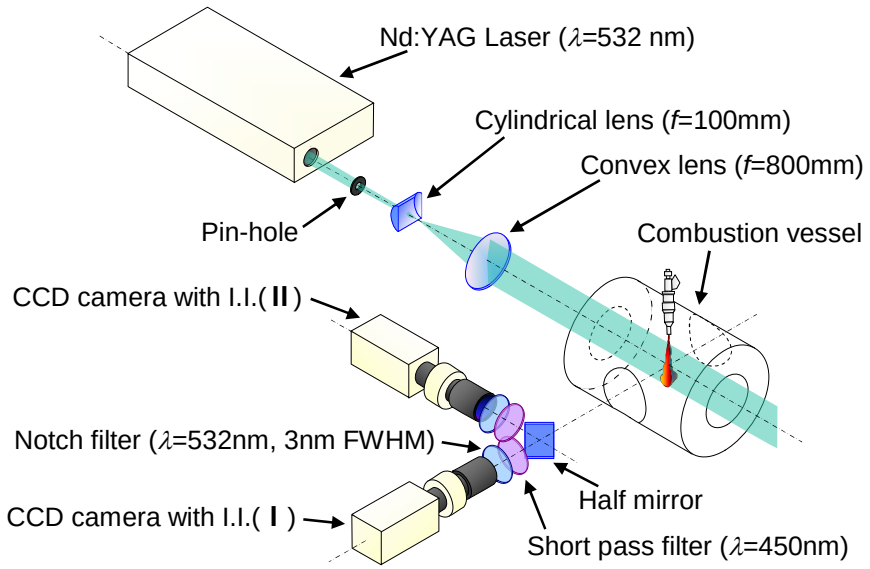

Property of test fuel

軽油 → すす生成量が多過ぎる．

↓

Fuel:N-heptane

レーザ光の減衰が著しく，またシート光とカメラまでのすすにより，LIIシグナルも大幅に減衰する．

Density at 298K	[kg/m^3]	680
Boiling point	[K]	372
Kinematic viscosity	[mm^2/s]	0.584
Lower calorific value	[MJ/kg]	47.8
Cetane number		56
Stoichiometric A/F	[kg/kg]	15.1

Experimental condition

Ambient gas temperature	T_{amb} [K]	900		
Ambient gas density	ρ_{amb} [kg/m^3]	16.2		
Ambient oxygen concentration	X_{O2} [%]	17, 21		
Nozzle orifice diameter	d [mm]	0.2		
Injection pressure drop	ΔP_{inj} [MPa]	40	70	100
Set injection duration	Δt_{inj} [ms]	3.2	2.65	2.1
Injection quantity	Q_{inj} [mg]	18.3		

f_v and d_p distribution (P_{inj}=70MPa)

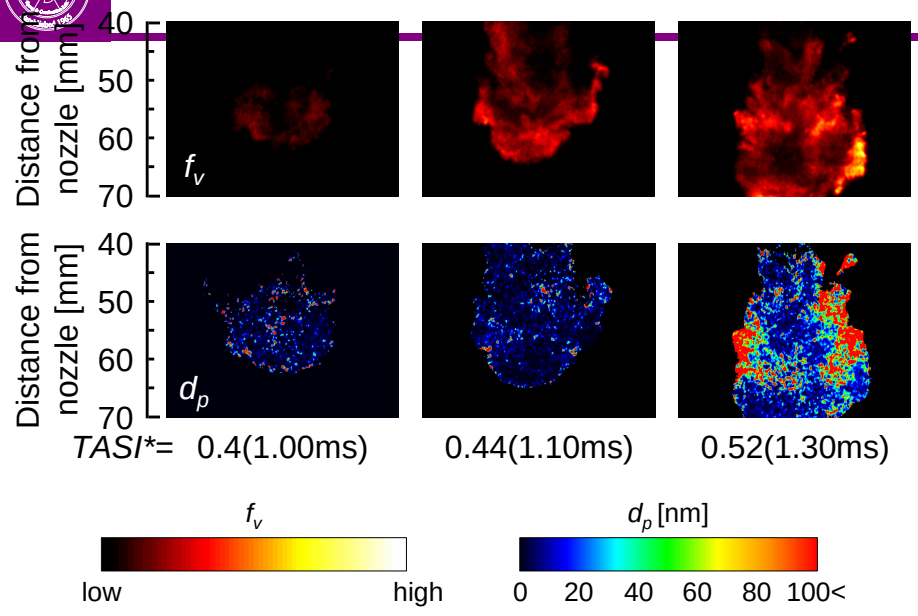

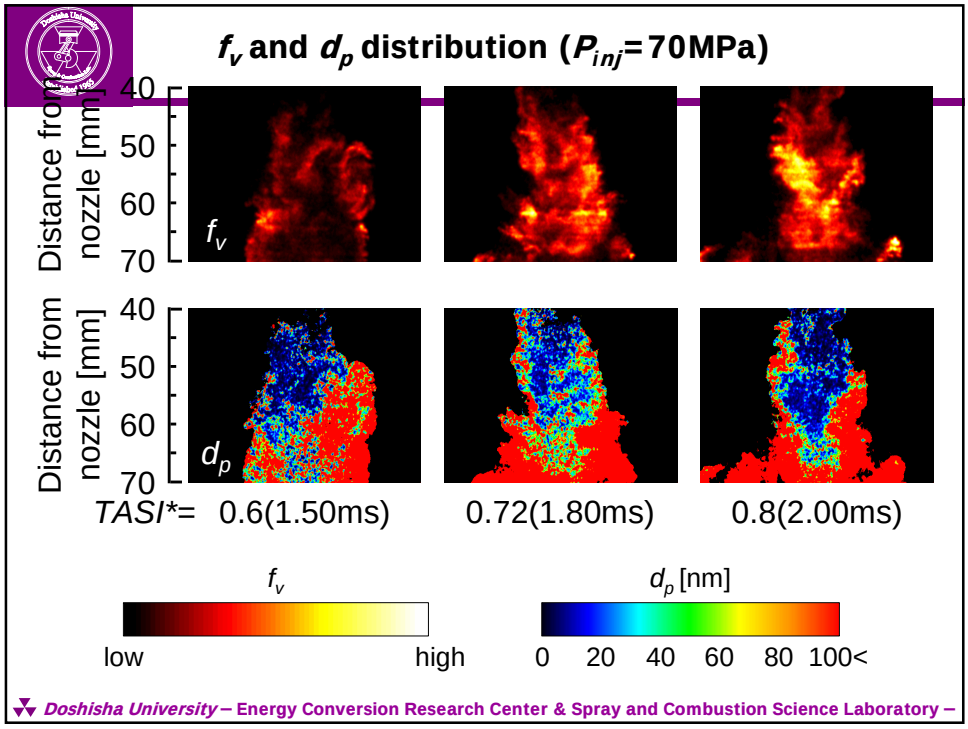
f_v and d_p distribution (P_{inj}=70MPa)
Distance from nozzle [mm]
40
50
60
70
f_v
d_p
TASI*= 0.6(1.50ms)
0.72(1.80ms)
0.8(2.00ms)
f_v
low
high
d_p [nm]
0 20 40 60 80 100<
Doshisha University – Energy Conversion Research Center & Spray and Combustion Science Laboratory –

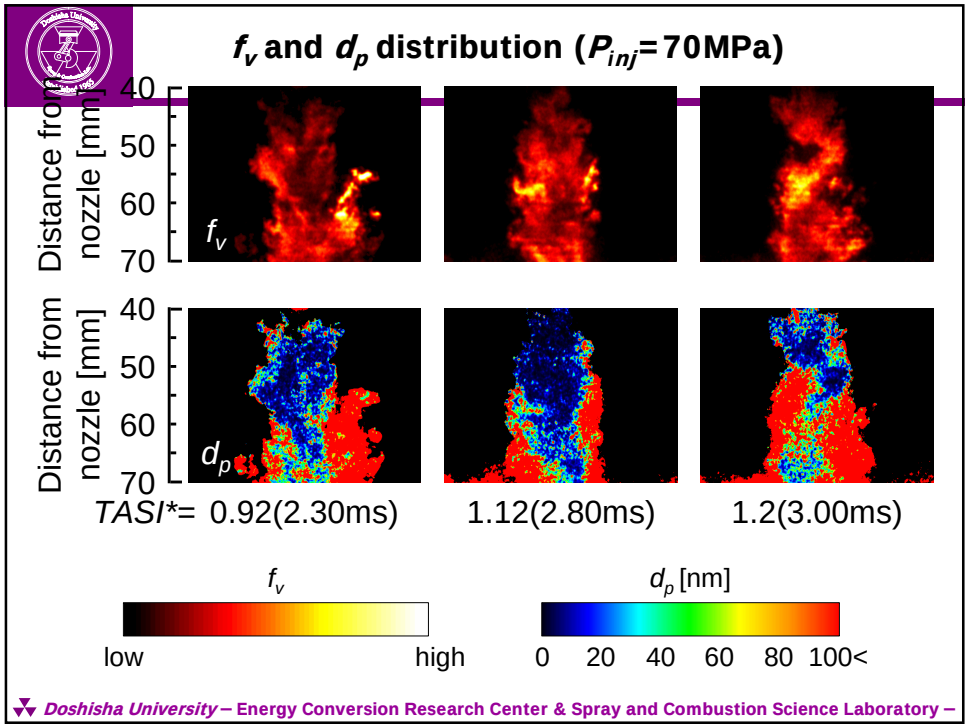
f_v and d_p distribution (P_{inj}=70MPa)
Distance from nozzle [mm]
40
50
60
70
f_v
d_p
TASI*= 0.92(2.30ms)
1.12(2.80ms)
1.2(3.00ms)
f_v
low
high
d_p [nm]
0 20 40 60 80 100<
Doshisha University – Energy Conversion Research Center & Spray and Combustion Science Laboratory –

燃料噴射圧力の影響 (上段：Δp_{inj}=40MPa，下段：100MPa)

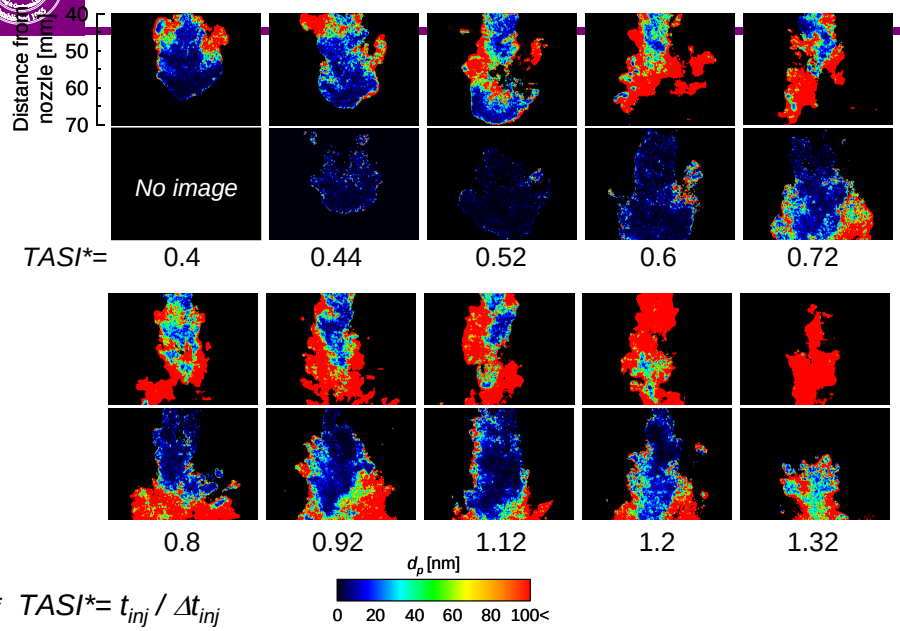

* $TASI^* = t_{inj} / \Delta t_{inj}$

雰囲気酸素濃度の影響 (上段：X_{o2}=21％，下段：17％)

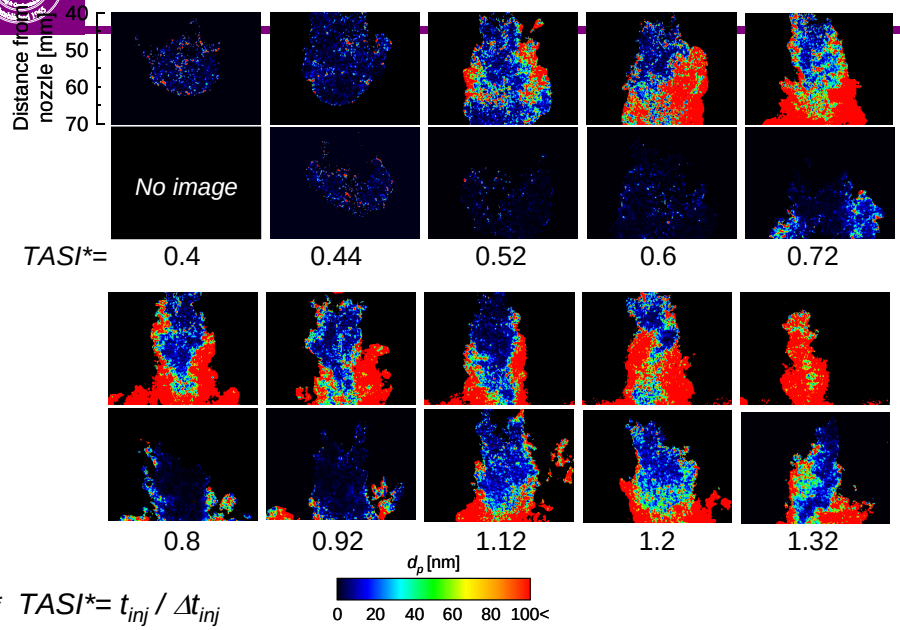

* $TASI^* = t_{inj} / \Delta t_{inj}$

Conclusion

- すす生成開始直後は，生成領域の全域を10～20nm程度の小さな粒子が占め，拡散的燃焼期間への移行に伴い，噴霧外縁付近から大粒子へと成長する．
- 上流側で生成された小粒径のすすは下流に向かうに従い，凝集や表面反応により成長し，大粒子化する．
- 大粒子径のすすは噴霧外縁付近に多く分布し，噴霧中心軸付近は小さなすす粒子で占められる．
- 噴射圧力が増加するに従い，大粒子径のすすが生成し始める位置は下流へと遷移し，その時期は噴射時期後半へと移行する．
- 雰囲気酸素濃度の低下は，噴霧火炎内部で生成されるすす粒子の成長を抑制し，すすの小粒径化をもたらす．

Experimental conditions

Fuel		n-Heptane
Ambient gas temperature	T_{amb} [K]	800 900 1200
Ambient gas density	ρ_{amb} [kg/m^3]	16.2
Ambient oxygen concentration	X_{O2} [%]	13 17 21
Nozzle orifice diameter	d [mm]	0.2
Injection pressure drop	ΔP_{inj} [MPa]	70
Injection duration	Δt_{inj} [ms]	2.5
Injection quantity	Q_{inj} [mg]	18.3

Distribution of soot volume fraction and soot particle diameter in diesel jet flame obtained by Time-resolved LII

fuel: n-heptane, T_{amb}=900[K], ρ_{amb}=16.2[kg/m³], X_{o2}=21%, ΔP_{inj}=70[MPa]

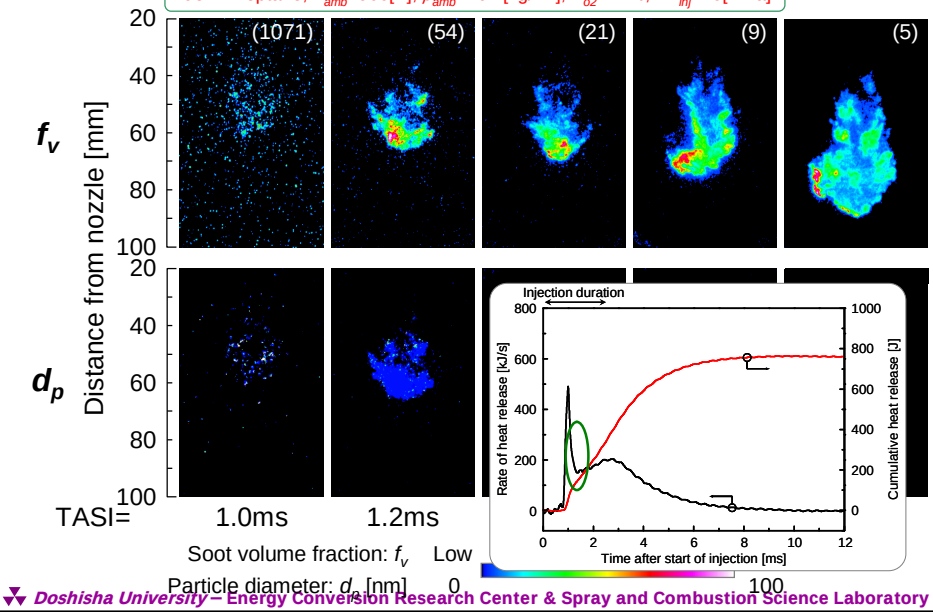

Distribution of soot volume fraction and soot particle diameter in diesel jet flame obtained by Time-resolved LII

fuel: n-heptane, T_{amb}=900[K], ρ_{amb}=16.2[kg/m³], X_{o2}=21%, ΔP_{inj}=70[MPa]

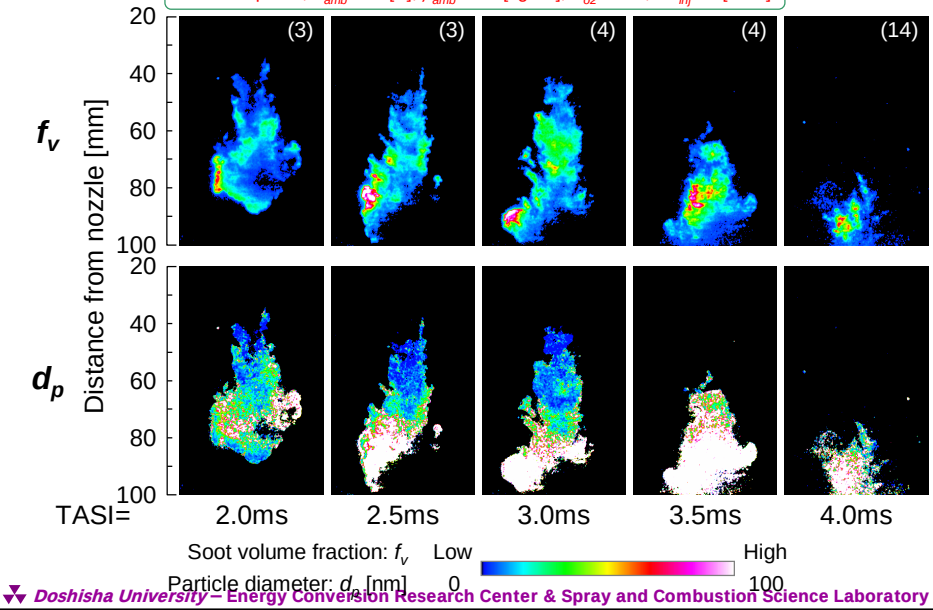

Doshisha University – Energy Conversion Research Center & Spray and Combustion Science Laboratory –

Distribution of soot volume fraction and soot particle diameter in diesel jet flame obtained by Time-resolved LII

fuel: n-heptane, ρ_{amb}=16.2[kg/m³], X_{o2}=21%, ΔP_{inj}=70[MPa]

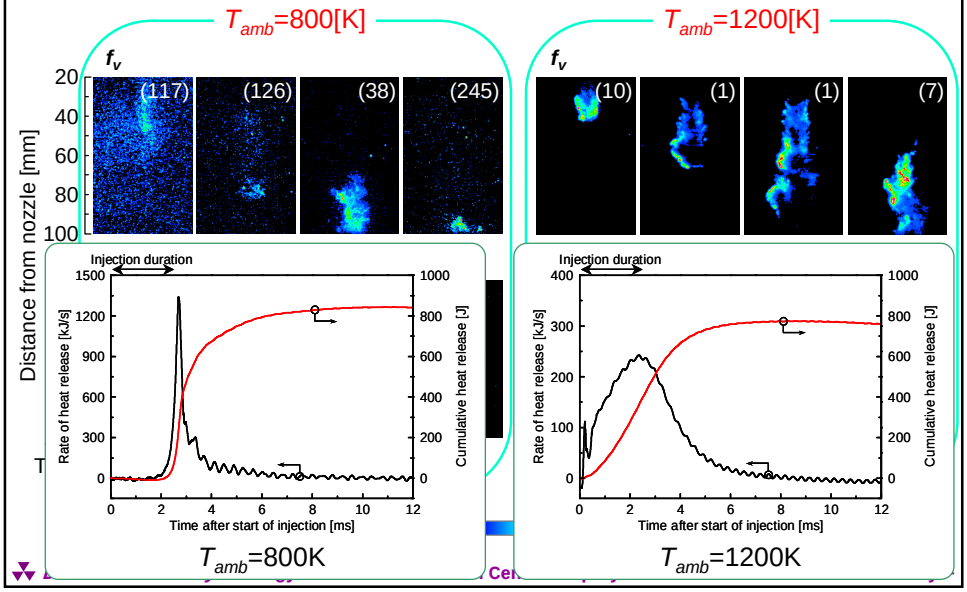

Distribution of soot volume fraction and soot particle diameter in diesel jet flame obtained by Time-resolved LII

fuel: n-heptane, T_{amb}=900[K], ρ_{amb}=16.2[kg/m³], X_{o2}=13%, ΔP_{inj}=70[MPa]

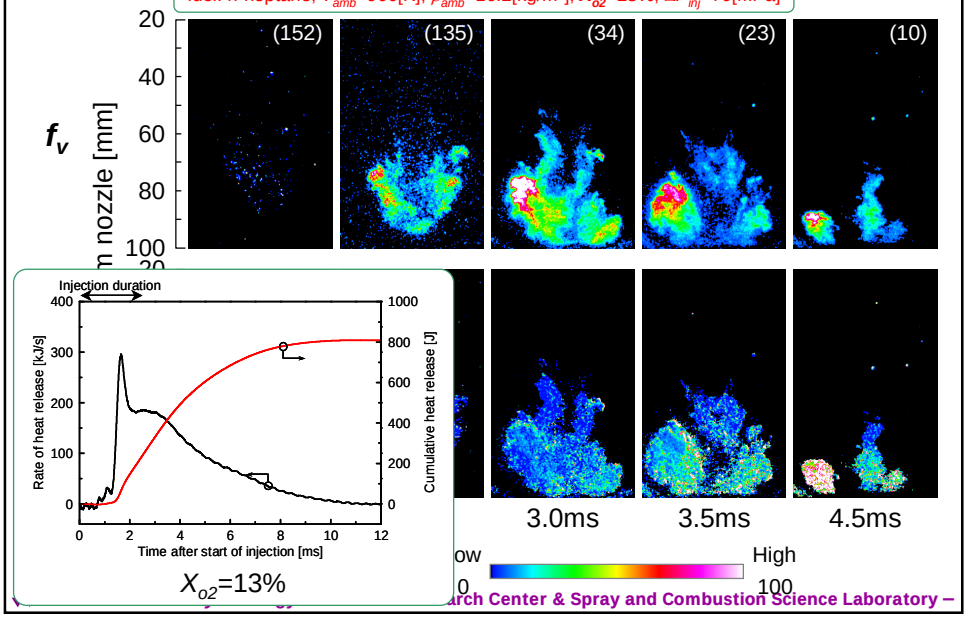

Integrated LII intensity and characteristic particle diameter

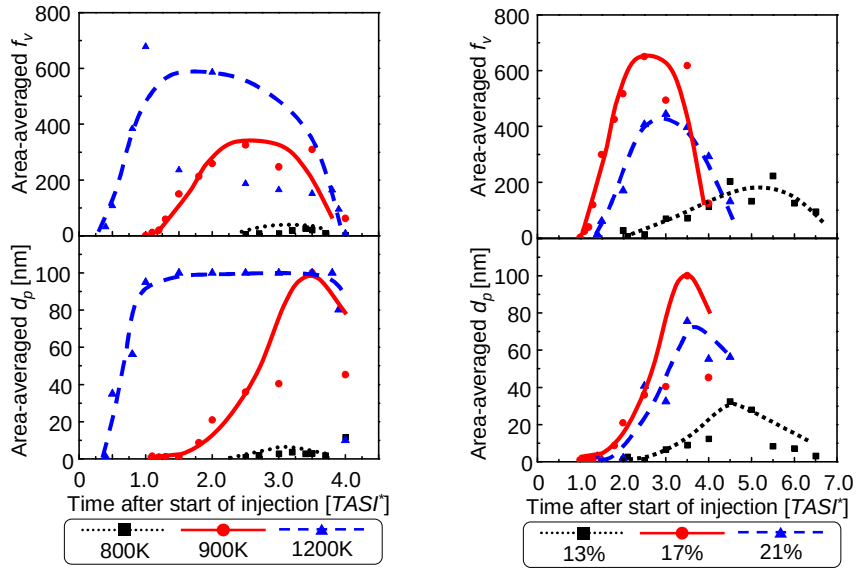

Conclusions

(1) 予混合的燃焼期間の終盤に生成した微小なすす粒子は燃焼の進行とともに噴霧下流部へ拡がり，噴霧先端･外縁部で大粒子径のすすが高濃度で分布する．

(2) 雰囲気温度の低下に伴い，大幅にすす濃度が減少し，粒子径もLIIシグナルが検出される全期間において微小となる．

(3) 雰囲気酸素濃度が低下すると，噴霧火炎が肥大化することにより，すす生成領域が拡大する．また，雰囲気酸素濃度の低下に伴い，すす粒子の生成･成長が緩慢となることで，粒子径およびすす濃度はともに減少する．

Effect of flame temperature on calculated diameter

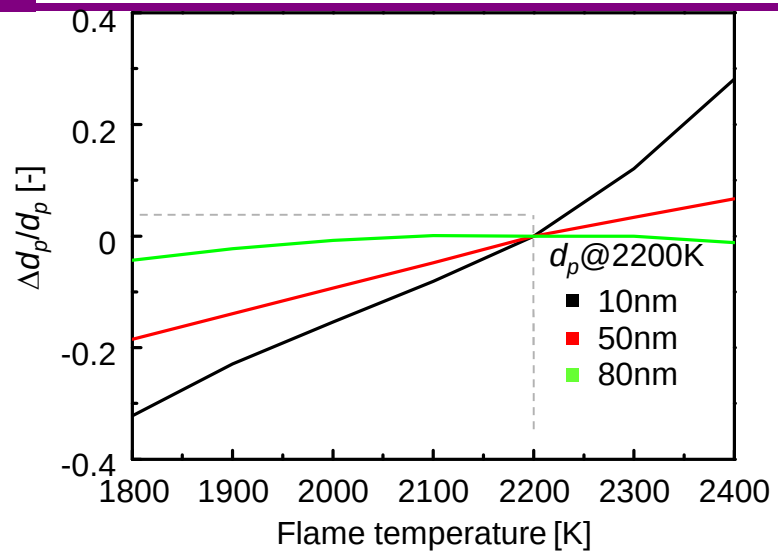

P_{amb}=4.1MPa, Laser fluence=0.67J/cm^2

Effect of laser fluence on calculated diameter

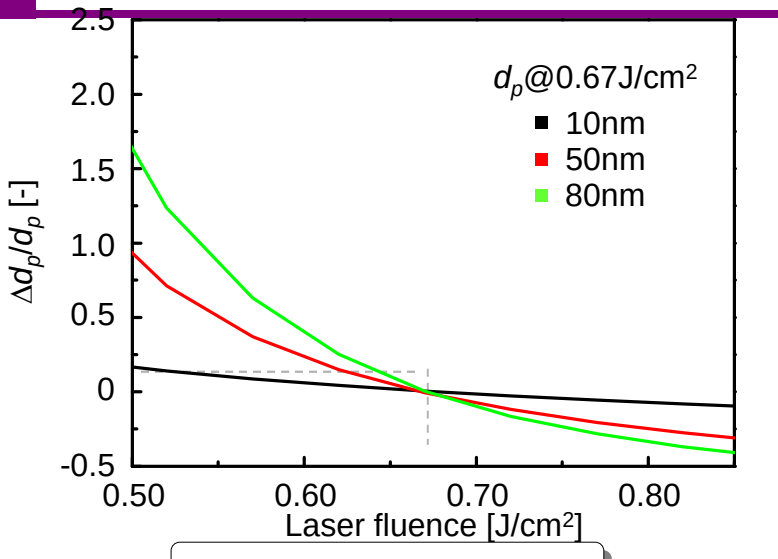

P_{amb}=4.1MPa, T_{flame}=2200K

Log-normal fitting of soot particle

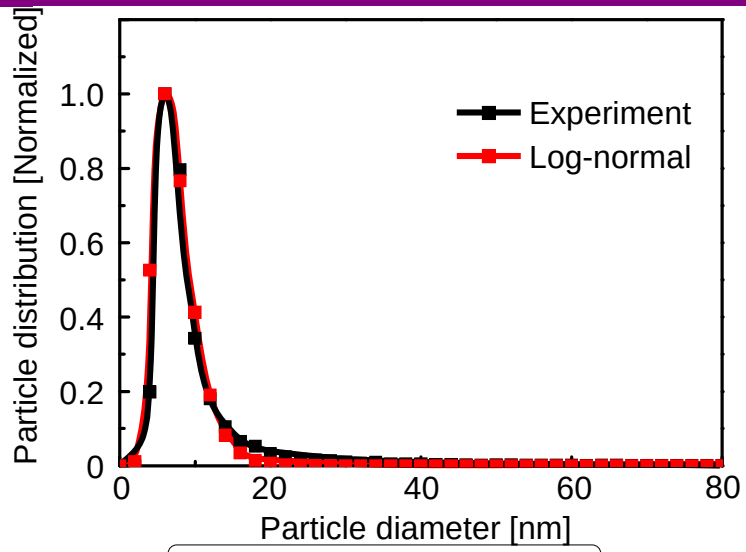

TASI=0.8ms, σ_g=1.45, D_g=7

Relative error of D_{mn} to D_{TIRE}

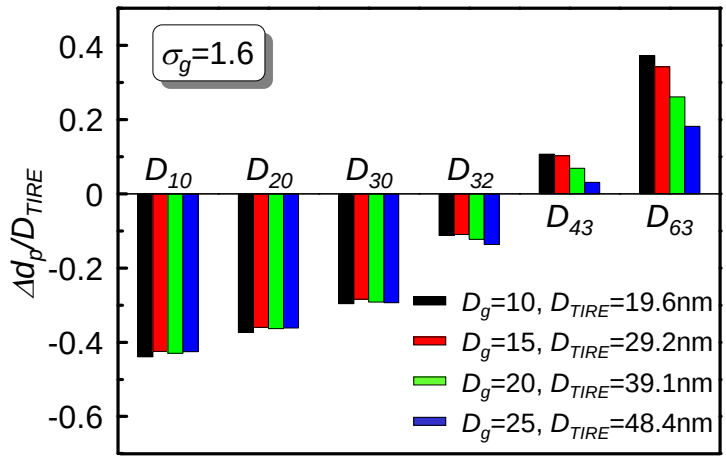

Temporal changes in particle size distribution for n-heptane

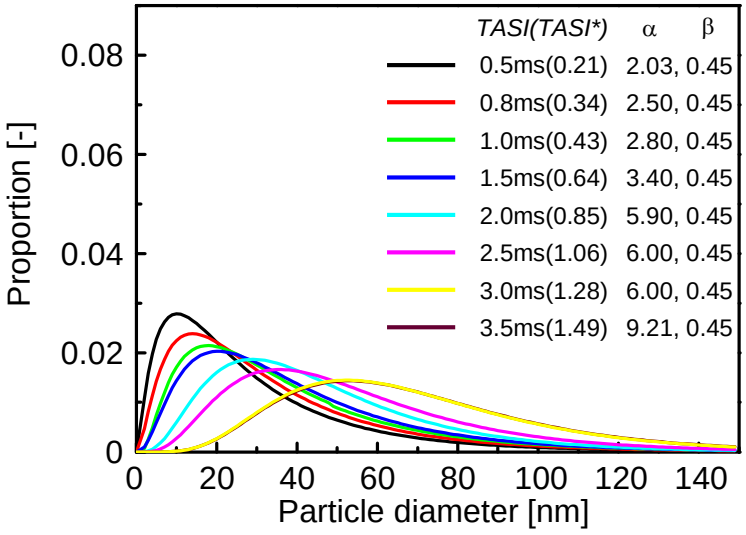

Temporal changes in particle size distribution for DGE

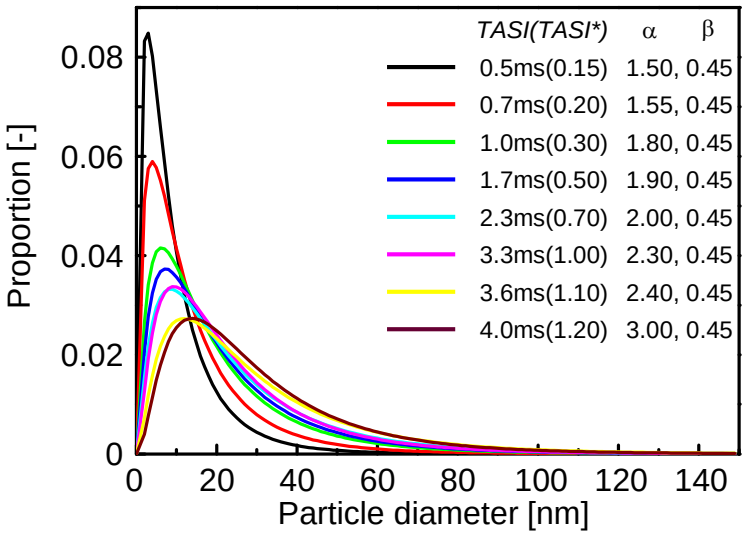

Time-Resolved LIIの問題点

- 検査領域中（画像ピクセル中）に粒度分布が存在する場合．見積もられる平均粒子径は概ねD_{32}と一致するが，粒度分布によって若干異なる．
- より定量的な結果を得るには噴霧火炎内部の局所的な温度情報が必要とされる．
- 下図のように凝集体の構造が異なる場合，算出される粒子径　？？？

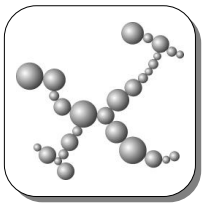

- point contact
- loose structure

$A_p = \sum_n A_{pp}$

A_{pp} = primary particle surface

measured diameter
=
mean primary particle diameter

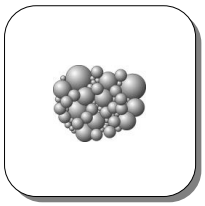

- compact
- dense structure

A_p = “enwrapped” surface of the agglomerate

measured diameter
=
“heat transfer diameter”

as equivalent diameter